Long- and short-range electron–hole exchange interaction in different types of quantum dots

Jun-Wei Luo[1]**, Gabriel Bester**[2,3] **and Alex Zunger**[1]

[1] National Renewable Energy Laboratory, Golden, CO 80401, USA
[2] Max Planck Institute for Solid State Research, D-70569 Stuttgart, Germany
E-mail: g.bester@fkf.mpg.de

Abstract. The electron–hole (e–h) exchange interaction leads to the splitting of the exciton into a pair of bright and a pair of dark states. This bright–dark—or singlet–triplet—exciton splitting was historically calculated as the sum of a long-range (LR) and a short-range (SR) component. Using a numerical atomistic approach, we are able to calculate the exchange integrals as a function of the e–h range of interaction *S*, revealing the 'internal' structure of the integrals. We apply this procedure to thickness-fluctuation GaAs∕AlGaAs quantum dots (QDs), self-assembled InAs∕GaAs QDs and colloidal InAs QDs. We find a heterogeneous situation, where the SR component contributes 10, 20–30 and 20–50% to the total e–h exchange splitting, which is in the range of 10, 100 and 10 000 μeV, for the three types of QDs, respectively. The balance between SR and LR is found to depend critically on the size, shape and type of structure. For all types of QDs we find, surprisingly, a range of interaction, close to the physical dimension of the structures, contributing to a reduction of the integral's magnitude. These results highlight the complexity of the exchange interaction, warning against simplified models, and establish the basic features of the nature and origin of dark–bright excitonic splitting in QDs.

[3] Author to whom any correspondence should be addressed.

Contents

1. Introduction

Electron–hole (e–h) interactions in semiconductor quantum dots (QDs) are manifested by a direct Coulomb part, constituting the 'excitonic-binding energies' (typically 0.01–0.5 eV) [1], as well as a Coulomb exchange interaction, constituting the 'dark–bright splitting', $_X$ (typically 0.000 01–0.005 eV) [2]–[4]. The latter interaction—due to the coupling of electron with hole spins—is important for many applications of QDs utilizing the spin degree of freedom in an optical setting [5
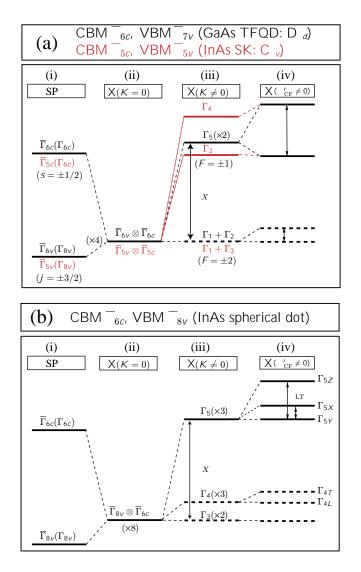
(e.g. equation (1)) becomes obvious from the size dependence of $_X$. For InP [11] and InAs [12], a dependence of $_X$ R^{-2} was found experimentally in contrast to the $_X$ R^{-3} dependence of equation (1). Furthermore, recent experiments on CdSe nanocrystals [10] highlight the discrepancy between exciton models such as that in equation (1) and experiments that call for a more comprehensive theory.
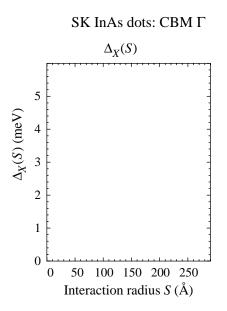
In this work, we wish to establish a description of the e–h exchange bright–dark splitting in QDs that reveals the relative importance of SR and LR effects and their dependence on size, shape and type of structure. This approach will be applied to the three leading forms of semiconductor QDs, with their attendant shapes, compositions and geometries; namely, (i) self-assembled QDs (e.g. InAs in GaAs), (ii) thickness fluctuation QDs (TFQDs, e.g. GaAs in AlGaAs) and (iii) colloidal QDs (e.g. InAs in chemical colloidal suspensions). To this end, we will use an atomistic approach to directly calculate the value of the e–h exchange energies [3, 13] and analyze the results as a function of the range of interaction included in the calculation of the integrals. We find for all three different types of dots a significant contribution from LR interactions. We also find a surprising non-monotonic behavior of the exchange interaction with increasing e–h interaction radius that we explain by an interface effect. This analysis establishes the basic features of the nature and origin of dark–bright excitonic splitting in QDs.

2. Symmetry analysis of exciton states in three prototypical quantum dots (QDs)

1. *Self-assembled (Stranski-Krastanov (SK)) QDs* are grown epitaxially under strain conditions leading to island (dot) formation [14]. The QDs are strained, embedded in a (usually) smaller lattice constant material such as InGaAs in GaAs, and have a shape resembling a lens or truncated cone.

2. TFQDs are created by a monolayer fluctuation in the width of a quantum well. In our case (and most experimental cases), the TFQDs are given by the one monolayer fluctuation of a nominally 10-monolayer thick $GaAs/Al_{0.3}Ga_{0.7}$

(a) CBM $\overline{\Gamma}_{6c}$, VBM $\overline{\Gamma}_{7v}$ (GaAs TFQD: D_d)
CBM $\overline{\Gamma}_{5c}$, VBM $\overline{\Gamma}_{5v}$ (InAs SK: C_v)

(i)	(ii)	(iii)	(iv)
SP	$X(K=0)$	$X(K \neq 0)$	$X(\Gamma'_{CF} \neq 0)$

Γ_4

$\overline{\Gamma}_{6c}(\Gamma_{6c})$
$\overline{\Gamma}_{5c}(\Gamma_{6c})$
$(s = \pm 1/2)$

$\Gamma_5 (\times 2)$
Γ_2
$(F = \pm 1)$

X

$(\times 4)$ $\overline{\Gamma}_{6v} \otimes \overline{\Gamma}_{6c}$
$\overline{\Gamma}_{5v} \otimes \overline{\Gamma}_{5c}$

$\Gamma_1 + \Gamma_2$
$\Gamma_1 + \Gamma_3$
$(F = \pm 2)$

$\overline{\Gamma}_{6v}(\Gamma_{8v})$
$\overline{\Gamma}_{5v}(\Gamma_{8v})$
$(j = \pm 3/2)$

(b) CBM $\overline{\Gamma}_{6c}$, VBM $\overline{\Gamma}_{8v}$ (InAs spherical dot)

(i)	(ii)	(iii)	(iv)
SP	$X(K=0)$	$X(K \neq 0)$	$X(\Gamma'_{CF} \neq 0)$

Γ_{5Z}

$\overline{\Gamma}_{6c}(\Gamma_{6c})$

$\Gamma_5 (\times 3)$

LT

Γ_{5X}
Γ_{5Y}

X

$\overline{\Gamma}_{8v} \otimes \overline{\Gamma}_{6c}$
$(\times 8)$

$\Gamma_4 (\times 3)$
$\Gamma_3 (\times 2)$

Γ_{4T}
Γ_{4L}

$\overline{\Gamma}_{8v}(\Gamma_{8v})$

Figure 1. Schematic of the evolution of the exciton states for (a) self-embedded InAs∕GaAs QDs (text in red) and GaAs TFQD (text in black) and (b) spherical InAs QDs. From the left to the right columns are the single-particle conduction

SK InAs dots: CBM Γ

$\Delta_X(S)$

Figure 2. (a) Unscreened ($\bar{\epsilon} = 1$) exchange energy $\Delta_X(S)$ for lens-shaped InAs self-assembled QDs with 250 Å diameter and three different heights, h, as a function of interaction radius S. (b) Percentage $\Delta_X(S)/\Delta_X(S = \infty)$ of the total

Table 1. Screened and unscreened e–h exchange energy splittings (Δ_X, see figure 1) in μeV and Coulomb energy Σ_{coul} in meV for three types of QD. The SR component, the total magnitude and the percentage of the SR part of the bright–dark exchange splittings are tabulated.

| | | $\Delta_X(S)$ (μeV) | | | | | | $\Sigma_{coul}(S)$ (meV) | | | |
| | | Screened | | | Unscreened | | | Screened | | Unscreened | |
Dot type	Dot size	SR	Total	Ratio (%)	SR	Total	Ratio (%)	SR	Total	SR	Total
SK	h20	35.5	262.4	13.5	80.8	3841.7	2.1	0.169	24.9	0.437	371.8
	h35	20.4	197.0	10.4	46.3	2898.7	1.6	0.100	21.4	0.254	313.9
	h50	8.4	97.8	8.5	19.0	1453.1	1.3	0.039	16.2	0.105	239.9
TFQDs	(200 × 200)	2.8	8.8	31.8	7.3	115.1	6.3	0.012	11.1	0.034	136.6
	(400 × 200)	2.0	7.2	27.8	5.2	85.7	6.1	0.008	9.6	0.025	118.3
	(400 × 400)	1.6	5.2	19.2	4.1	61.2	6.7	0.007	9.0	0.022	112.1
Colloidal	R10	16 750	30 581	54.8	17 655	98 654	17.9	25.2	244.6	21.4	1585.0
	R15	5090	13 358	38.1	6327	66 779	9.5	8.1	156.3	8.3	1154.9
	R20	1879	7034	26.7	2559	45 240	5.7	3.2	105.7	3.9	892.3
	R25	589	3095	19.0	870	24 394	3.6	1.4	75.9	2.3	728.0
	R30	307	2093	14.7	470	18 684	2.5	0.8	60.6	1.5	620.0

total interaction is given in per cent. We added the direct Coulomb interactions Σ_{coul} to the table to highlight the differences between direct and exchange integrals. The analysis of table 1 and figures 2–4 leads to five main conclusions.

1. The *total* (i.e. evaluated for $S = \infty$) e–h exchange energy Δ_X in colloidal InAs QDs is at least one order of magnitude larger than in self-assembled InAs/GaAs SK QDs, which, in turn, is at least an order of magnitude larger than in TFQDs. This reveals that the degree of state localization enhanced by quantum confinement is a principal factor in increasing the exchange interactions. In colloidal InAs QDs, electrons and holes are strongly localized inside the QD's interior by the large conduction and valence band offsets, whereas TFQDs have small band offsets of $\sim$10 meV (along in-plane directions). The combination of small-sized objects and deep confinement potentials in colloidal QDs, versus large-sized objects with small band offsets in TFQDs, lead to the nearly four orders of magnitude difference in Δ_X. The ratio between unscreened and screened total exchange energy Δ_X is close to their bulk static dielectric constant ($\epsilon_0^{InAs} = 15.2$ and $\epsilon_0^{GaAs} = 12.4$ [23]) in SK InAs/GaAs QDs and TFQDs; however, in colloidal InAs QDs it decreases fast from 8.9 to 3.2 as QD size decreases from $R = 30$ Å to $R = 10$ Å. The latter effect is the consequence of the size-dependent SR contribution in colloidal structures.

2. For all three types of QDs studied here, we find a balanced situation where both the SR and the LR parts contribute to the exchange integral. Moreover, we find that the balance between SR and LR components changes as a function of size and type of QDs. In general, quantum confinement increases not only the total exchange energy, Δ_X, but also the SR component in all three systems. However, using the sole argument of the degree

of localization of the wavefunctions to draw conclusions on the SR–LR balance would be

5. The e–h exciton binding energy Δ_{coul} is naturally dominated by the LR direct Coulomb interaction. Table 1 shows that in both SK QDs and TFQDs, the SR contribution to total Δ_{coul} is less than 1%. The SR direct Coulomb component increases as QD size decreases. In colloidal InAs QDs, the SR contribution increases from 1 to 10% as QD size decreases from $R = 30\,\text{Å}$ to $R = 10\,\text{Å}$. In the envelope-function approximation, assuming an infinite potential barrier at the surface of the QD and a size-independent dielectric constant, one would expect the size-scaling exponent $\gamma_{coul} \simeq 1$ ($\Delta_{coul} \propto R^{-\gamma_{coul}}$). We find $\gamma_{coul} = 1.4$ for InAs QDs (see table 1). The deviations from the $1/R$ scaling are primarily due to the electron and hole wavefunctions 'spilling out' of the QD as the size becomes smaller [26].

6. Summary

We have calculated the e–h exchange bright–dark splitting for three different common types of QD using an atomistic methodology. The numerical method employed enables us to truncate the interaction after a certain cut-off radius and study the SR and LR nature of the interaction. We first show that from group theory arguments the expected splittings are qualitatively different for all three types of QD. We then analyze the numerical results to draw several conclusions. (i) The e–h integrals vary by more than three orders of magnitude for the three different types of QD as a consequence of the differences in sizes and confinement potentials. (ii) Quantum confinement increases the SR contribution to the integral within one QD type. Across QD types, no such simplification can be made and factors such as shape and the underlying band structure become relevant. For instance, TFQDs have a larger SR component than SK QDs. (iii) For SK QDs and TFQDs, we observe an overshoot of $\delta_X(S)$ for an interaction radius close to the Wigner–Seitz radius. We related this effect to the degree of macroscopic anisotropy in the structure. No overshoot is observed in spherical structures. (iv) For the three types of QD, we observe a pronounced maximum in $\delta_X(S)$ at an interaction radius S representing the physical dimension of the QDs. This result shows that the exchange integral is not a purely cumulative quantity (when the interaction radius is increased the magnitude of the integral increases), but has positive as well as negative contributions. We attribute the pronounced maximum to the effect of wavefunction distortions at the interface of the QDs. (v) We find for colloidal InAs QDs a scaling of the exchange integrals $\propto R^{-2.2}$ and of the direct Coulomb integrals $\propto R^{-1.4}$.

Acknowledgment

References

[1] Brus L E 1984 *J. Chem. Phys.* **80** 4403
[2] Bayer M, Ortner G, Forchel A, Hawrylak P and Fafard S 2002 *Physica* E **13** 123
[3] Bester G, Nair S and Zunger A 2003 *Phys. Rev.* B

12

[6] Knox R S 1963 *Theory of Excitons in Solid State Physics* ed F Seitz and D Turnbull (New York: Academic)

[7] Takagahara T 1993 *Phys. Rev.* B **47** 4569

[8] Efros A L, Rosen M, Kuno M, Nirmal M, Norris D J and Bawendi M 1996 *Phys. Rev.* B **54** 4843

[9] Gupalov S and Ivchenko E L 2000 *Fiz. Tverd. Tela* **42** 1976
Gupalov S and Ivchenko E L 2000 *Phys. Solid State* **42** 2030

[10] Liptay T J, Marshall L F, Rao P S, Ram R J and Bawendi M G 2007 *Phys. Rev.* B **76** 155314

[11] Micic O I, Cheong H M, Fu H, Zunger A, Sprague J R, Mascarenhas A and Nozik A J 1997 *J. Phys. Chem.* B **101** 4904

[12] Banin U 1997 *Superlattices Microstruct.* **22** 559

[13] Franceschetti A, Wang L W, Fu H and Zunger A 1998 *Phys. Rev.* B **58** R13367

[14] Bimberg D, Grundmann M and Ledentsov N N 1999 *Quantum Dot Heterostructures* (New York: Wiley)

[15] Luo J W, Bester G and Zunger A 2009 *Phys. Rev.* B **79** 125329

[16] Califano M, Bester G and Zunger A 2003 *Nano Lett.* **3** 1197

[17] Koster G F, Dimmock J O, Wheeler R G and Satz H 1963 *Properties of the Thirty-Two Point Groups* (Cambridge, MA: MIT Press)

[18] Rossler U and Trebin H-R 1981 *Phys. Rev.* B **23** 1961

[19] Wang L W and Zunger A 1995 *Phys. Rev.* B **51** 17398

[20] Wang L W, Kim J and Zunger A 1999 *Phys. Rev.* B **59** 5678

[21] Franceschetti A, Fu H, Wang L-W and Zunger A 1999 *Phys. Rev.* B **60** 1819

[22] Resta R 1977 *Phys. Rev.* B **16** 2717

[23] Madelung O 1996 *Semiconductors—Basic Data* 2nd revised edn (Berlin: Springer)

[24] BenDaniel D J and Duke C B 1966 *Phys. Rev.* **152** 683

[25] Luo J W, Li S S, Xia J B and Wang L W 2006 *Appl. Phys. Lett.* **88** 143108

[26] Franceschetti A and Zunger A 1997 *Phys. Rev. Lett.* **78** 915